Modulating the voltage sensor of a cardiac potassium channel shows antiarrhythmic effects

Yangyang Lin[a,b,c,1], Sam Z. Grinter[d,e,f,1], Zhongju Lu[g,1], Xianjin Xu[d,1], Hong Zhan Wang[g], Hongwu Liang[a,b,c], Panpan Hou[a,b,c], Junyuan Gao[g], Chris Clausen[g], Jingyi Shi[a,b,c], Wenshan Zhao[a,b,c], Zhiwei Ma[d,f], Yongfeng Liu[a,b,c], Kelli McFarland White[a,b,c], Lu Zhao[a,b,c], Po Wei Kang[a,b,c], Guohui Zhang[a,b,c], Ira S. Cohen[g,2], Xiaoqin Zou[d,e,f,h,2], and Jianmin Cui[a,b,c,2]

[a]Department of Biomedical Engineering, Washington University, St. Louis, MO 63130; [b]Center for the Investigation of Membrane Excitability Disorders, Washington University, St. Louis, MO 63130; [c]Cardiac Bioelectricity and Arrhythmia Center, Washington University, St. Louis, MO 63130; [d]Dalton Cardiovascular Research Center, University of Missouri, Columbia, MO 65211; [e]Institute for Data Science and Informatics, University of Missouri, Columbia, MO 65211; [f]Department of Physics and Astronomy, University of Missouri, Columbia, MO 65211; [g]Department of Physiology and Biophysics, Stony Brook University, Stony Brook, NY 11794; and [h]Department of Biochemistry, University of Missouri, Columbia, MO 65211

Edited by Lily Yeh Jan, University of California, San Francisco, CA, and approved April 9, 2021 (received for review November 25, 2020)

Cardiac arrhythmias are the most common cause of sudden cardiac death worldwide. Lengthening the ventricular action potential duration (APD), either congenitally or via pathologic or pharmacologic means, predisposes to a life-threatening ventricular arrhythmia, Torsade de Pointes. I_{Ks} (KCNQ1+KCNE1), a slowly activating K^+ current, plays a role in action potential repolarization. In this study, we screened a chemical library in silico by docking compounds to the voltage-sensing domain (VSD) of the I_{Ks} channel. Here, we show that C28 specifically shifted I_{Ks} VSD activation in ventricle to more negative voltages and reversed the drug-induced lengthening of APD. At the same dosage, C28 did not cause significant changes of the normal APD in either ventricle or atrium. This study provides evidence in support of a computational prediction of I_{Ks} VSD activation as a potential therapeutic approach for all forms of APD prolongation. This outcome could expand the therapeutic efficacy of a myriad of currently approved drugs that may trigger arrhythmias.

KCNQ1 | I_{Ks} | C28 | voltage sensor domain | antiarrhythmia

I_{Ks} (KCNQ1+KCNE1), a slowly activating delayer rectifier in the heart, is important in controlling cardiac action potential duration (APD) and adaptation of heart rate in various physiological conditions (1). The I_{Ks} potassium channel has slow activation kinetics, and the activation terminates cardiac action potentials (APs) (2). This channel is formed by the voltage-gated potassium (K_V) channel subunit KCNQ1 and the regulatory subunit KCNE1. The association of KCNE1 drastically alters the phenotype of the channel, including a shift of voltage dependence of activation to more positive voltages, a slower activation time course, a changed ion selectivity, and different responses to drugs and modulators (3–6). Similar to other K_V channels, KCNQ1 has six transmembrane segments, S1 to S6, in which S1 to S4 form the voltage-sensing domain (VSD), while S5 and S6 form the pore domain (PD); four KCNQ1 subunits comprise the KCNQ1 channel (7, 8). KCNQ1 and I_{Ks} channels are activated by voltage. The VSD in response to membrane depolarization changes conformation, triggered by the movements of the S4 segment that contains positively charged residues (9–15). This conformational change alters the interactions between the VSD and the pore, known as the VSD–pore coupling, to induce pore opening (12–15).

The ventricular APD depends on the balance of outward and inward currents flowing at plateau potentials. The outward currents include the delayed rectifiers I_{Kr} and I_{Ks}, while the inward currents include a persistent sodium current (I_{NaP}) (16). Specific mutations in any of these channel proteins that cause a reduction in outward current or increase in inward current are associated with congenital long QT syndrome (LQTS). The QT interval is the time between the initial depolarization of the ventricle until the time to full repolarization. LQTS is a condition in which the APD is abnormally prolonged, predisposing the afflicted patients to a lethal cardiac arrhythmia called Torsades de Pointes (TdP) (17). In fact, mutations in multiple genes that alter the function of various ion channels have been associated with LQTS (18). There is also a much more prevalent problem called acquired LQTS (aLQTS) that is most often associated with off target effects of drugs. Many drugs are marketed with a QT prolongation warning, and the drug concentrations that can be used therapeutically are limited by this potentially lethal side effect. Some effective drugs have been removed from the market (19) because of QT prolongation, and others are abandoned before clinical trials even began. Therefore, aLQTS is costly for the pharmaceutical industry both in drug development (to avoid this side effect) and when it results in removal from the market of compounds that have effectively treated other diseases (20, 21). At present, the I_{Kr} (HERG) potassium channel (20) and the phosphoinositide 3-kinase (PI3K) (22, 23) have been identified as the most prominent off targets of these drugs for the association with aLQTS.

We hypothesized that in LQTS, the normal heart function can be restored and QT prolongation prevented by compensating for

Significance

C28, a chemical compound identified by computational screening, selectively facilitates voltage-dependent activation of a cardiac potassium ion channel, I_{Ks}. This compound reverses drug-induced prolongation of the electric signals across the cardiac cell membrane known as action potentials (APs) but minimally affects the normal AP at the same dosage. This outcome supports a computational prediction that enhancing voltage-dependent activation of I_{Ks} could be a potential therapy for AP prolongation. This therapy would increase the safety and expand the therapeutic efficacy of many currently approved drugs that induce AP prolongation, which can trigger life-threatening cardiac arrhythmias.

Author contributions: Y. Lin, G.Z., I.S.C., X.Z., and J.C. designed research; Y. Lin, S.Z.G., Z.L., X.X., H.Z.W., H.L., P.H., J.G., C.C., J.S., W.Z., Z.M., Y. Liu, and K.M.W. performed research; Y. Lin, S.Z.G., Z.L., X.X., H.Z.W., H.L., P.H., J.G., C.C., W.Z., Y. Liu, K.M.W., L.Z., P.W.K., and G.Z. analyzed data; and G.Z., I.S.C., X.Z., and J.C. wrote the paper.

Competing interest statement: J.S. and J.C. are cofounders of a startup company VivoCor LLC, which is targeting I_{Ks} for the treatment of cardiac arrhythmia.

This article is a PNAS Direct Submission.

[1]Y.L., S.Z.G., Z.L., and X.X. contributed equally to the work.

[2]To whom correspondence may be addressed. Email: ira.cohen@stonybrook.edu, ZouX@missouri.edu, or jcui@wustl.edu.

This article contains supporting information online at https://www.pnas.org/lookup/suppl/doi:10.1073/pnas.2024215118/-/DCSupplemental.

Published May 14, 2021.

the change in net current from any of the channels produced by the myocyte; all that is required is that a reasonable facsimile of normal net current flow be restored. We applied this approach to aLQTS based on a computational study to show that a shift of voltage-dependent activation of I_{Ks} to more negative voltages would increase I_{Ks} during ventricular APs; this increase of I_{Ks} would revert drug-induced APD prolongation to normal. More importantly, a change in I_{Ks} voltage-dependent activation might affect the normal APD to a much smaller degree because of its slow activation kinetics in healthy ventricular myocytes, thereby posing minimal risk of cardiac toxicity on its own. To apply this approach experimentally, we needed a compound that could specifically shift the voltage dependence of I_{Ks} activation. Previous studies showed that the benzodiazepine R-L3 (24) and polyunsaturated fatty acids (25) activate I_{Ks} channels, while more recently, rottlerin was shown to act similarly to R-L3 (26). However, the effects of these compounds on I_{Ks} are complex, likely through binding to more than one site in the channel protein instead of simply acting on voltage-dependent activation (24, 27, 28). In addition, these compounds showed poor specificity for I_{Ks}, also affecting other ion channels in the heart (27, 29, 30), which make these compounds unsuitable to test our hypothesis. Recently, we have identified CP1 as an activator for I_{Ks}, which mimics the membrane lipid phosphatidylinositol 4,5-bisphosphate (PIP_2) to mediate the VSD–pore coupling (13, 31). CP1 enhances I_{Ks} primarily by increasing current amplitude with some shift of voltage dependence of activation, which is not suitable for our test either.

In this study, we identified a compound, C28, using an approach that combines in silico and experimental screening, that interacts with the KCNQ1 VSD and shifts voltage dependence of VSD activation to more negative voltages. C28 increases both exogenously expressed I_{Ks} and the current in native cardiac myocytes. As predicted by computational modeling, C28 can prevent or reverse the drug-induced APD prolongation back to normal while having a minimal effect on the control APD at the same concentration in healthy cardiac myocytes. This study demonstrates that the KCNQ1 VSD can be used as a drug target for developing a therapy for LQTS, and C28 identified in this study may be used as a lead for this development. Furthermore, our results provide support for the use of docking computations based on ion channel structure and cellular physiology, in combination with functional studies based on molecular mechanisms, as an effective approach for rational drug design.

Results

C28 Shifts Voltage Dependence of KCNQ1 and I_{Ks} to More Negative Voltages. In a previous study, we showed that, during activation of the KCNQ1 VSD (Fig. 1*A*), residue E160 in the S2 helix interacts with positively charged residues in S4 as they move toward the extracellular side of the membrane in response to depolarization of the membrane potential, and these interactions could be modified by extracellular compounds to alter channel gating (9). This result suggested that the KCNQ1 VSD could serve as a target for developing antiarrhythmic drugs. To identify a compound that would bind to the pocket near these interactions, we used our MDock docking software (32–34) to screen in silico a compound library targeting the VSD of KCNQ1, as described in the *Materials and Methods* (*SI Appendix, Supplementary Materials*). We used the Available Chemical Database (Molecular Design Ltd.) as the compound library, which consists of over 200,000 organic compounds. The in silico screening produced 53 candidates, which were further screened experimentally using voltage clamp. The compound C28 was further docked onto the recently solved cryogenic electron microscopy (cryo-EM) structure of human KCNQ1 (8) (Fig. 1 *A* and *B*). C28 was found to cause a shift in the voltage dependence of activation for both KCNQ1 and I_{Ks} channels (Figs. 1 and 2).

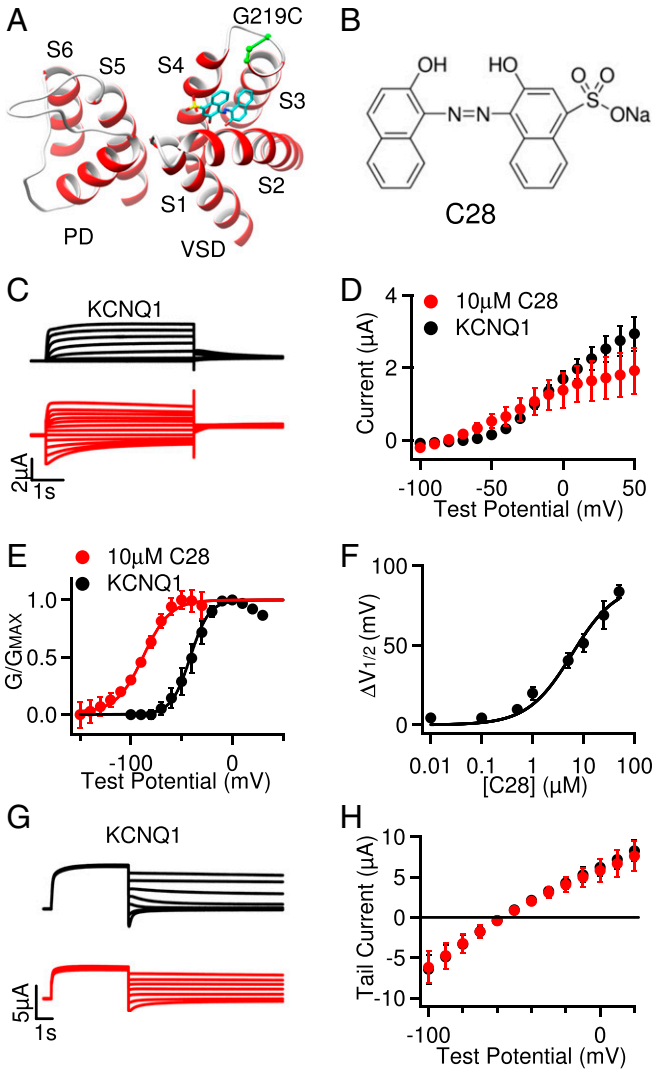

Fig. 1. Effects of C28 on KCNQ1 opening. (*A*) Cryo-EM structure of KCNQ1 (Protein Database Bank [PDB] entry: 6uzz) docking with C28 (cyan, yellow, and red sticks). G219C (green) was covalently labeled with Alexa488 in VCF experiments. S1 to S6: transmembrane helices. The VSD (S1 to S4) and the PD (S5 to S6) are from neighboring subunits. (*B*) C28 molecule. (*C*) Currents of KCNQ1 (black) and with C28 (10 μM, red) at various test voltages (see *D*). The potentials before and after test pulses were −80 and −40 mV, respectively. (*D*) Steady-state current-voltage relations with current amplitudes at the end of test pulses shown in *C*. $P > 0.05$ between control and C28 at all voltages, unpaired Student's *t* test. (*E*) G–V relations. Solid lines are fits to the Boltzmann relation with $V_{1/2}$ and slope factor (millivolts) for control: −41.4 ± 1.4 and 9.3 ± 1.3 and for 10 μM C28: −87.7 ± 1.4 and 13.3 ± 1.4. (*F*) The change of $V_{1/2}$ of G–V relations depends on C28 concentration, with EC_{50} of 7.6 μM. (*G*) Reversal potential measurements. KCNQ1 channels were activated at 40 mV and then currents were tested at −100 to 20 mV. Holding potential: −80 mV. Control: black, with C28 (10 μM): red. (*H*) Peak tail currents in relation to the test voltages. The currents reversed at potentials (millivolts): −58.2 ± 0.8 for control (black) and −57.1± 1.1 for 10 μM C28 (red). All data in this figure and subsequent figures are mean ± SEM, $n = 3$ to 15 unless otherwise specified.

We measured the modulation of the KCNQ1 channel activation by C28 at various concentrations. The current amplitude was increased at low voltages with the application of C28, but the changes were not significant (Fig. 1 *C* and *D*), while the voltage dependence of activation, measured as the conductance–voltage (G–V) relation, was shifted to more negative voltages (Fig. 1*E*). These results suggest that C28 enhanced channel activation by

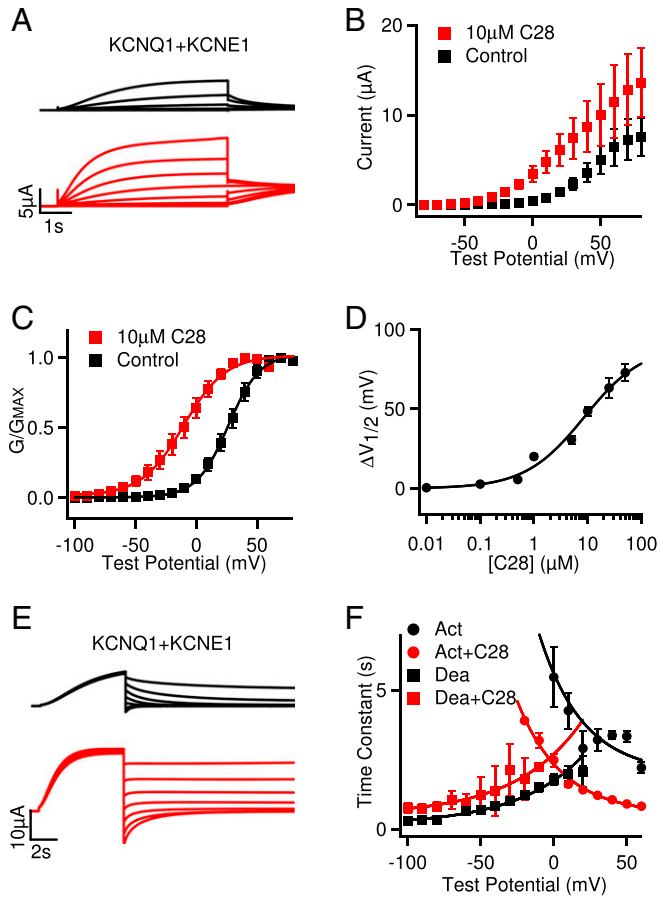

Fig. 2. Effects of C28 on I_{Ks} opening. (*A*) I_{Ks} (black) and with C28 (10 μM, red) at various voltages (see *B*). The potentials before and after test pulses were −80 and −40 mV, respectively. (*B*) Steady-state current-voltage relations. $P < 0.05$ between control and C28 at voltages −50 to +20 mV, unpaired Student's *t* test. (*C*) G–V relations. Solid lines are fits to the Boltzmann relation with $V_{1/2}$ and slope factor (millivolts): 26.4 ± 0.6 and 13.1 ± 0.5 for control, and −10.4 ± 1.3 and 17.3 ± 1.3 for 10 μM C28. (*D*) G–V shifts in response to C28. EC_{50} is 5.9 μM. (*E*) I_{Ks} deactivation. The channels were activated at 60 mV and then tested at −100 to 40 mV. Control: black, with C28 (10 μM): red. (*F*) Voltage dependence of activation (Act) and deactivation (Dea) time constants of I_{Ks} in control and 10 μM C28. The time constants were obtained by exponential fitting to current traces. Solid lines are exponential fits to the data. $P < 0.05$ between control and C28 at all voltages, unpaired Student's *t* test.

altering KCNQ1 voltage dependence. The shift of G–V relation could be as large as −90 mV, and the EC_{50} for the shift was 7.6 μM (Fig. 1*F*). C28 did not alter the reversal potential of KCNQ1 channels, suggesting that K^+ selectivity of the channel was not affected by C28 (Fig. 1 *G* and *H*). These results are consistent with our docking computations of C28 interacting with the KCNQ1 VSD (Fig. 1*A*).

We then examined the effects of C28 on I_{Ks} channels. We found that the KCNQ1 and I_{Ks} channel inhibitor XE991 could still inhibit the I_{Ks} channel in the presence of C28 (*SI Appendix*, Fig. S1 *A* and *B*), and the result indicates that C28 did not elicit any change in the endogenous currents in oocytes. C28 also increased current amplitude (Fig. 2 *A* and *B*), and the effects could be washed out (*SI Appendix*, Fig. S1*C*). C28 shifted the G–V relation of the I_{Ks} channel to more negative voltages (Fig. 2*C*), similarly to the result for KCNQ1. At 10 μM C28, the G–V shift was ∼−37 mV for I_{Ks} as compared to ∼−46 mV for KCNQ1 (Figs. 1*E* and 2*C*). The shift of the I_{Ks} G–V relation showed a similar dependence on C28 concentrations as that of KCNQ1, with the EC_{50} at 5.9 μM (Fig. 2*D* and *SI Appendix*, Fig. S1*D*), as compared to 7.6 μM for KCNQ1 (Fig. 1*F*). Interestingly, the VSD of the KCNQ1 channel activates in two steps, first to the intermediate state and then to the activated state, and the KCNQ1 channel opens predominantly when the VSD is at the intermediate state, while the I_{Ks} channel opens exclusively when the VSD is at the activated state (35, 36). This mechanism is manifested in the result that the G–V relation of KCNQ1 was in a more negative voltage range than the G–V relation of I_{Ks} (Figs. 1*E* and 2*C*). Therefore, the similar shift of G–V relations for both KCNQ1 and I_{Ks}, caused by C28, suggests that C28 alters VSD activation to both intermediate and activated states, which is supported by the direct studies of VSD activation (see below). C28 accelerated activation kinetics of I_{Ks} and reduced the rate of deactivation to a small degree (Fig. 2 *E* and *F*).

C28 Modulates KCNQ1 VSD Activation by Interacting with the VSD. The effects of C28 on the voltage dependence of the KCNQ1 and I_{Ks} opening are consistent with our docking result that C28 may bind to the VSD of the channels and alter VSD activation. We further validated this mechanism by first measuring the effects of C28 on VSD activation and then identifying the residues in the KCNQ1 VSD that may interact with C28. To directly examine if C28 modulates the VSD, we measured VSD activation and channel opening in response to voltage changes using voltage-clamp fluorometry (VCF) (Fig. 3). The fluorophore, Alexa 488 C5 maleimide, labeling C219 in the VSD (Fig. 1*A*) of the KCNQ1 pseudo–wild-type (psWT) channels (carrying mutations C214A/G219C/C331A), reported VSD movements, while the ionic current reported pore opening (10–14, 36). The mutations in the psWT avoid nonspecific labeling of native Cys214 and Cys331. These mutations and fluorophore labeling had a small effect on KCNQ1 activation, shifting the voltage dependence of channel activation by ∼9 mV to more negative voltages in the absence of C28 (Figs. 1*E* and 3 *A* and *B*). However, similar to the WT KCNQ1 channel, C28 also facilitated opening of psWT KCNQ1 channels by shifting the G–V relation to more negative voltages (Fig. 3*B*). C28 caused a striking change of the fluorescence emission, such that instead of an increasing of fluorescence in response to VSD activation, the fluorescence decreased in response to VSD activation upon the wash in of C28 (Fig. 3*C*). The change of fluorescence during each voltage pulse is a result of the environmental change surrounding the fluorophore due to VSD movements in response to voltage (13, 14). The fluorophore was labeled close to the target pocket in our in silico screening (C219, Fig. 1*A*). C28 reversed the direction of the fluorescence change during VSD activation (Fig. 3 *C* and *D*), supporting the hypothesis that C28 binds to the targeted pocket in the VSD (Fig. 1*A*) and alters the fluorophore in relation to its environment during VSD movements by changing either the fluorophore or the conformation of the VSD. In fact, C28 might have affected the fluorophore severely, such that, at C28 concentrations higher than 1.5 μM used in these experiments (Fig. 3), the VCF recordings were not stable and could not be completed. We measured the steady-state voltage dependence of the change of fluorescence emission, $\Delta F/F$ (Fig. 3 *D* and *E*), which increased with voltage in two distinct steps (Fig. 3*E*), reflecting the stepwise VSD movements of KCNQ1 from the resting state to the intermediate state and then to the activated state (9–12, 35–37). C28 shifted both components of the $\Delta F/F$–V relation to more negative voltages (Fig. 3*E*), consistent with similar C28 effects on both KCNQ1 and I_{Ks} openings (Figs. 1 and 2). These results indicate that C28 facilitates VSD activation.

To examine if C28 interacts with the KCNQ1 VSD, we first measured the effects of C28 on Kir1.1, which is a two-transmembrane–segment K^+ channel that contains a PD but not the VSD. C28 had no effect on Kir1.1 channels (*SI Appendix*, Fig. S2 *A* and *B*), consistent with the hypothesis that C28 only

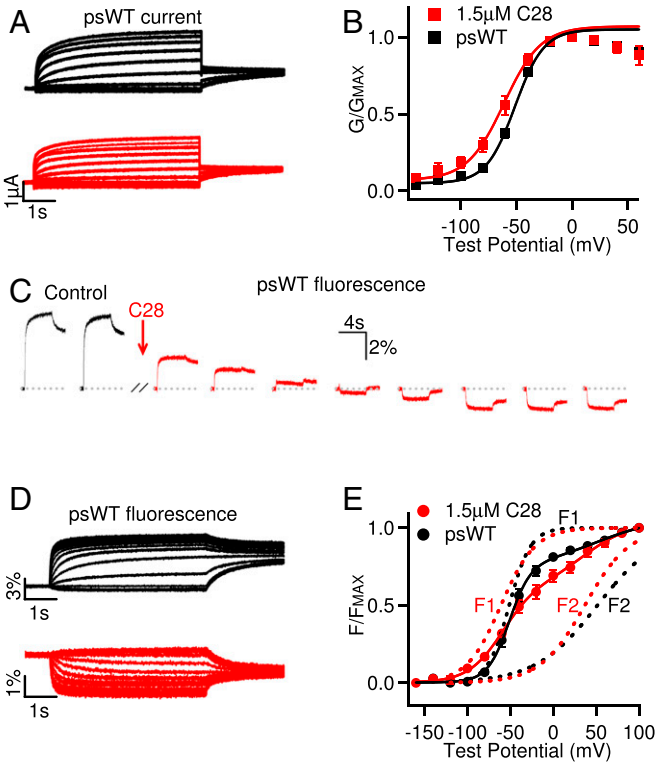

Fig. 3. C28 enhances KCNQ1 VSD activation. (*A*) Currents of psWT KCNQ1 (black) and with C28 (1.5 μM, red) at various test voltages (see *B*). The potentials before and after test pulses were −80 and −40 mV, respectively. (*B*) G–V relations. Solid lines are fits to the Boltzmann relation with $V_{1/2}$ and slope factor (millivolts): −50.4 ± 0.9 and 13.9 ± 0.7 for psWT, and −59.7 ± 1.1 and 15.2 ± 1.4 for C28. $n = 7$. (*C*) Fluorescence change of psWT in response to voltage pulses to 40 mV (−80 mV before and −40 mV after the test pulse, pulse interval: 40 s) altered direction upon C28 (1.5 μM) application. (*D*) Fluorescence changes of psWT KCNQ1 (black) and with C28 (1.5 μM, red) in response to the voltage protocols from the same oocyte in *A*. (*E*) Normalized fluorescence–voltage relation. The curves are fits with double Boltzmann functions (F1 and F2) with the $V_{1/2}$ and the slope factor. $V_{1/2}$ (millivolts): F1 −51.9 ± 1.1 and F2 49.1 ± 2.0 for psWT; F1 −60.6 ± 1.4 and F2 39.1 ± 3.3 for C28. Slope factor (millivolts): F1 12.2 ± 0.5 and F2 36.0 ± 0.8 for psWT, and F1 21.5 ±1.4 and F2 26.5 ±3.1 for C28. $n = 5$. The statistical significance of differences in $V_{1/2}$ between C28 and control were tested using unpaired Student's *t* test; $P < 0.001$ for G–V (*B*), and $P < 0.005$ and $P < 0.05$ for F1 and F2, respectively (*E*).

interacts with the VSD. All K_V channels have VSDs that share a similar structure, containing four transmembrane helices S1 to S4. However, we found that, unlike its action on KCNQ1, C28 did not alter voltage-dependent activation of the Shaker K^+ channel (*SI Appendix*, Fig. S2 *C* and *D*). To test if this result derives from a specificity of C28 to the KCNQ1 VSD, we studied the KTQ and KTV channels, which are comprised of the two-pore–domain channel TWIK-related, acid-sensitive K^+ 3 (TASK3) fused with the KCNQ1 and K_V1.2 VSD, respectively (38). TASK3 itself lacks a VSD so that its opening is not dependent on voltage (39), but Lan et al. (38) demonstrated that the fused VSD induces voltage-dependent gating in the KTQ and KTV channels (Fig. 4 *A*–*D*). We found that C28 shifted voltage-dependent activation of the KTQ channel, which is composed of TASK3 fused with the KCNQ1 VSD, to more negative voltages and suppressed the amplitude of the current (Fig. 4 *A* and *B*). However, C28 had no effect on the KTV channel, which is composed of TASK3 fused with the Kv1.2 VSD (Fig. 4 *C* and *D*). These results suggest that the VSD of KCNQ1 specifically renders C28 sensitivity to the KTQ channel. The VSDs of Shaker and its ortholog Kv1.2 do not respond to C28.

To further validate the docking results, we identified the residues in the KCNQ1 VSD that are important for C28 modulation by mutagenesis studies. Docking of C28 onto the VSD pocket in the cryo-EM structure of human KCNQ1 (8) showed residues that may interact with C28 (Fig. 4*E* and *SI Appendix*, Fig. S3*A*). We mutated these residues to alanine (except for R228 to glutamine) and measured the shift of voltage-dependent activation of the mutant I_{Ks} channel at various C28 concentrations (Fig. 4*F*). The mutation of these residues increased the C28 concentration for half maximal shift of G–V relations, EC_{50}, and decreased the maximum amplitude of G–V shifts (Fig. 4*G*). These include arginine residues in S4 that are part of the voltage sensor, and some of the mutations altered voltage-dependent activation of I_{Ks} in the absence of C28 (*SI Appendix*, Fig. S3 *B*–*D*), supporting the idea that C28 binds to our targeted pocket and interferes with voltage sensor movements. A structural comparison

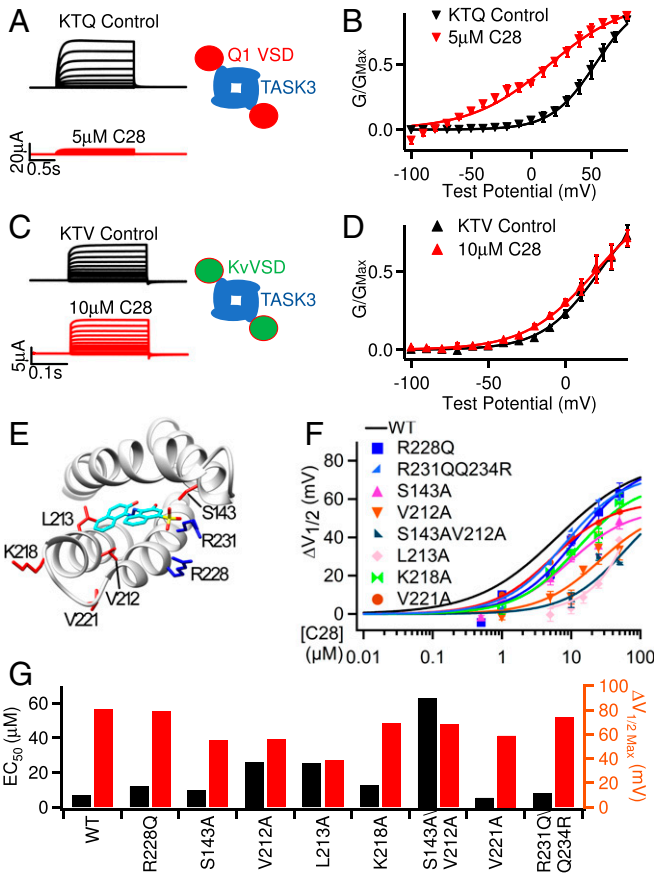

Fig. 4. Interactions of C28 with the VSD of KCNQ1. (*A* and *B*) C28 alters KTQ channel activation. KTQ is a fusion protein between the two-pore–domain channel TASK3 and KCNQ1 VSD (*Inset*). (*A*) Currents were elicited by voltage pulses from −100 to 80 mV with 20 mV increments from a holding potential of −80 mV. (*B*) G–V and Boltzmann fits (solid lines) with $V_{1/2}$ and slope factor (millivolts): 53.1 ± 2.5 and 18.4 ± 2.5 for control; 14.9± 8.2 and 32.8 ± 8.0 for C28. (*C* and *D*) C28 has no effect on KTV channel activation. KTV is a fusion protein between TASK3 and Kv1.2 VSD (*Inset*). In *C*, currents were elicited by voltage pulses from −100 to 40 mV with 20 mV increments. In *D*, G–V and Boltzmann fits (solid lines) with $V_{1/2}$ and slope factor (millivolts) for control (21.7 ± 4.0 and 18.5 ± 4.2) and for C28 (19.2± 3.8 and 22.5 ± 4.0). (*E*) Residues interacting with C28 based on molecular docking to the cryo-EM structure of human KCNQ1 (PDB entry: 6uzz). The S3 to S4 loop was missing in the cryo-EM structure, and we built it using MODELER (55). (*F*) G–V shift of mutant I_{Ks} in response to C28. Each data point was averaged from recordings in three to seven oocytes. The curve for WT is the same as in Fig. 2*D*. (*G*) Maximal G–V shift and EC_{50} for each mutation and WT.

between the VSDs of KCNQ1 and $K_V1.2$ (*SI Appendix*, Fig. S4 *A* and *B*) shows that the KCNQ1 VSD has short extracellular S1 to S2 and S3 to S4 loops, which expose the binding pocket completely to the extracellular solution. In addition, the residues that are important for C28 interaction in the KCNQ1 VSD are not conserved in the $K_V1.2$ VSD (*SI Appendix*, Fig. S4*B*). These structural differences may underscore the specificity of C28 for KCNQ1 and I_{Ks}.

C28 Enhances VSD–Pore Coupling in I_{Ks} Channels. The above results show that C28 activated KCNQ1 and I_{Ks} channels by shifting the voltage-dependent opening to more negative voltages (Figs. 1 and 2) because of the enhancement of VSD activation by C28 (Fig. 3) via interactions with the VSD (Fig. 4). However, C28 may activate I_{Ks} via an additional mechanism. The amplitude of I_{Ks} increased with C28 application at all voltages (Fig. 2 *A* and *B*). Even at very positive voltages, where the voltage-dependent activation was saturated, the I_{Ks} amplitude seemed to increase in the presence of C28 (Fig. 2*B*). This suggests an enhancement of the maximum conductance, in addition to the shift of the G–V relation. A change in the maximum conductance could be due to a change in the single-channel conductance. Since the total number of channels expressed in a cell is not expected to change with C28 application, the maximum conductance is proportional to the single-channel conductance. However, given that C28 binds to the VSD of I_{Ks} channels but not in the pore (Fig. 4), it is unlikely that C28 directly changed single-channel conductance of these channels. On the other hand, a change of the VSD–pore coupling could change the efficiency of pore opening in response to VSD activation to alter the maximum conductance. C28 may enhance the efficiency of VSD–pore coupling, such that the maximal open probability of each channel is increased to give rise to our observed results.

On the other hand, C28 did not increase the maximum conductance of KCNQ1 (Fig. 1 *C* and *D*). Then why does C28 show different effects on the maximum currents of KCNQ1 and I_{Ks}? It has been shown that the KCNQ1 channel can open when the VSD moves to either the intermediate or the activated states, resulting in two distinct open states, the intermediate open (IO) and the activated open (AO). For the KCNQ1 channel, IO is the predominant open state, whereas for the I_{Ks} channel AO is the exclusive open state, because the association of KCNE1 suppresses IO (35, 36). At the IO and AO states, the interactions between the VSD and the pore differ, resulting in different VSD–pore coupling (12). In addition, the VSD–pore coupling in KCNQ1 and I_{Ks} channels are dependent on the membrane lipid PIP_2 (13, 31), and KCNE1 association enhances PIP_2 binding to the channel (4, 36). These results demonstrate that the VSD–pore coupling mechanism differs in the KCNQ1 and I_{Ks} channels. Thus, C28 may show different effects on the maximum currents of KCNQ1 and I_{Ks} based on its differential effects on the IO and AO state. To test this idea, we examined if C28 affected the current amplitude of mutant KCNQ1 channels with the VSD arrested in either the intermediate state or the activated state (Fig. 5). The mutant KCNQ1 channels were stabilized in the IO and AO states, respectively, producing constitutive currents (Fig. 5 *A* and *B*, black) and no longer activated by voltage changes (10, 36, 40). Any C28 effect on the current amplitudes of these mutant channels should therefore be proportional to modulation of VSD–pore coupling. We found that C28 enhanced current amplitude in the channel with the VSD arrested in the activated state (Fig. 5 *A* and *B*) but not in the channel with the VSD arrested in the intermediate state (Fig. 5 *C* and *D*). These findings clearly show that C28 modulated VSD–pore coupling of the IO state and AO state differently. Since KCNQ1 and I_{Ks} conduct primarily at the IO and AO state, respectively, these results are consistent with the idea that in the I_{Ks} channel C28 binding to the VSD also affects the interactions between the VSD and the pore, resulting in changes of the VSD–pore coupling to alter the maximum conductance in I_{Ks} but not in KCNQ1.

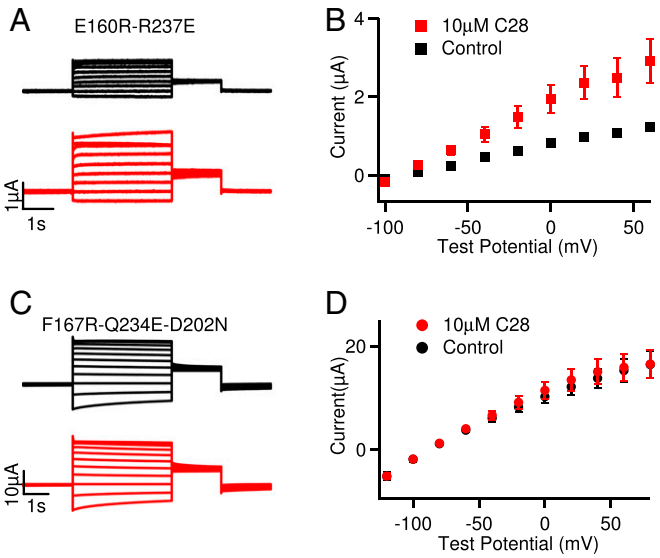

Fig. 5. Effects of C28 on KCNQ1 channels in the AO and IO states. (*A*) Current traces of KCNQ1 with mutations E160R-R237E, which arrested the VSD in the activated state and stabilized the channel at the AO state (36). Currents were recorded without (black) and with (red) 10 μM C28 at various voltages (see *B*). The voltage before and after the test pulses were −80 and −40 mV, respectively. (*B*) Steady-state current-voltage relations of KCNQ1 E160R-R237E mutant. (*C*) Current traces of KCNQ1 with mutations F167R-Q234E-D202N, which arrested the VSD at the intermediate state, thus the channels were stabilized at the IO state (10). Currents were recorded without (black) and with (red) 10 μM C28 at various voltages (see *D*). The voltage before and after the test pulses were −80 and −40 mV, respectively. (*D*) Current-voltage relations of KCNQ1 F167R-Q234E-D202N mutant. $P < 0.05$ in *B* but $P > 0.05$ in *D* between control and C28 at all voltages, using unpaired Student's *t* test.

C28 Reverts Drug-Induced APD Prolongation. Current antiarrhythmic drug therapy restores normal cardiac rhythm by inhibiting membrane ion conductance, which in turn alters the conduction velocity, varies the excitability of cardiac cells by changing the duration of the effective refractory period, and/or suppresses abnormal automaticity (41, 42). In a computational simulation of canine ventricular APs, we found that an increase of the I_{Ks} current by shifting its voltage dependence of activation to more negative voltages could reverse much of the prolongation of APD caused by the elimination of I_{Kr} (*SI Appendix*, Fig. S5*A*), while inducing only a small shortening in control conditions (*SI Appendix*, Fig. S5*B*). Similar effects of I_{Ks} current on APDs could be observed experimentally on isolated myocytes from the canine ventricle in the presence of dofetilide alone, in combination with C28 and with application of C28 alone (*SI Appendix*, Fig. S5 *C* and *D*).

With these encouraging preliminary studies, we further examined the effects of C28 on I_{Ks} and APs in cardiac myocytes. We first tested the effects of C28 on other ion channels that are also critical for shaping cardiac APs (16) (*SI Appendix*, Fig. S6). C28 did not show effects on the voltage dependence of voltage-gated Ca^{2+}, Na^+, or other K^+ channels (*SI Appendix*, Fig. S6 *A–D*). These results suggest that, although these channels have VSDs with a similar membrane topology to the KCNQ1 VSD, the specific structural features of the VSD in KCNQ1 and I_{Ks} channels may render it the specificity to its C28 interaction (*SI Appendix*, Fig. S4*B*). On the other hand, C28 activated the M-channel formed by KCNQ2/KCNQ3 with a smaller effect than KCNQ1

(*SI Appendix*, Fig. S7), which are expressed in neurons but share a more closely homologous VSD with KCNQ1 (43).

We then tested the effects of C28 on I_{Ks} and APs of guinea pig (GP) ventricular myocytes. We used low concentrations of C28 in order to determine the concentration range that might be effective in reducing drug-induced prolongation of APD but less effective in reducing the normal APDs. Varying concentrations of C28 (1 nM to 1 μM) shifted voltage dependence of the I_{Ks} channels in GP ventricular myocytes in a manner similar to those expressed in *Xenopus* oocytes, but in the GP myocytes, I_{Ks} seemed to be more sensitive to C28 (Figs. 2*D* and 6 *A* and *B*). This difference in drug action between oocytes and mammalian cells has been reported for other channels (44). C28 only modulated the currents that were sensitive to the I_{Ks} channel inhibitor Chromanol 293B but had no effect on currents that were not inhibited by Chromanol 293B (*SI Appendix*, Fig. S8 *A–C*), indicating that C28 specifically modified I_{Ks} channels in ventricular myocytes. Furthermore, in ventricular myocytes, C28 at these concentrations did not alter the maximum conductance of I_{Ks} in GP ventricular myocytes but increased I_{Ks} amplitude in the voltage range of the AP, primarily by shifting G–V to more negative voltages (Fig. 6 *A–C* and *SI Appendix*, Fig. S8*D*). C28 effectively reversed the prolongation of the APD caused by the I_{Kr} blocker (Moxifloxacin, Moxi) and by a PI3K inhibitor (PI-103) (Fig. 6 *D* and *E*). It has been shown that PI-103 decreases I_{Kr} and I_{Ks} currents, the L-type Ca^{2+} channel current $I_{Ca,L}$, and the peak Na^+ current I_{Na}, while it increases the persistent Na^+ current I_{NaP} (22). These results indicate that the enhancement of I_{Ks} currents by C28 stabilized APs with the alteration of multiple other ion channels. On the other hand, the same dosage of C28 had smaller or absent effects on the normal APD (Fig. 6*E* and *SI Appendix*, Fig. S8 *E* and *F*). Prolonged ventricular APs manifest in the whole heart as an increased QT interval in electrocardiogram (45). The effects of C28 on APD suggest that C28 should be effective at reducing or eliminating the drug-induced QT prolongation by shifting voltage dependence of I_{Ks} channel activation, while having little or no effect in control conditions.

It was shown that some congenital gain-of-function KCNQ1 mutations are associated with atrial fibrillation (46). While C28's enhancement of I_{Ks} is responsible for reducing drug-induced ventricular APD prolongation, is it prone to induce atrial fibrillation as well? To answer this question, we recorded APs in GP atrial myocytes in the presence of various concentrations of C28. The AP was not affected by C28 up to 1 μM (Fig. 6 *F* and

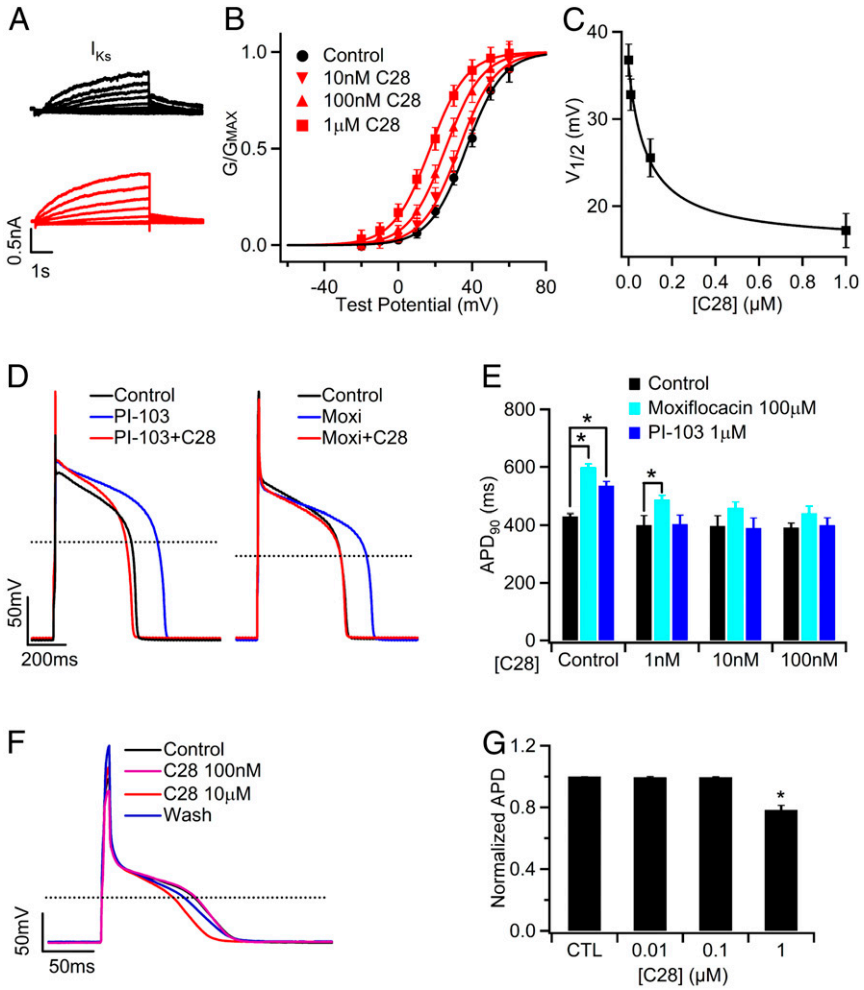

Fig. 6. C28 enhances I_{Ks} and stabilizes APs in GP ventricular and atrial myocytes. (*A*) I_{Ks} currents, measured as the Chromanol 293B sensitive currents (*SI Appendix*, Fig. S8 *A* and *B*), of control (black) and with C28 (100 nM, red) at various voltages (see *B*) from a ventricular myocyte. The voltage before and after the test pulses were −40 and −20 mV, respectively. (*B*) I_{Ks} G–V relations in various C28 concentrations. The lines are fits to Boltzmann equation. (*C*) $V_{1/2}$ of G–V relations versus C28 concentration. (*D*) C28 (100 nM) on APs in control and in the presence of PI-103 (1 μM) and Moxifloxacin (Moxi, 100 μM). (*E*) Effects of C28 on APD. $^*P < 0.05$, $n = 5$ to 44. (*F*) APs of a GP atrial myocyte recorded in control, C28 (100 nM and 10 μM), and after washout (Wash). The stimulus was 180 pA in amplitude and 10 ms in duration at 1 Hz frequency. (*G*) Effects of C28 on atrial APD. $^*P < 0.05$ compared to control, $n = 9$ to 12.

G), a concentration that is more than 100-fold higher than the concentration that was effective in reversing drug-induced prolongation of ventricular APD (Fig. 6*D*). This result indicates that C28 at a wide range of concentrations may alleviate LQTS symptoms without the risk of causing atrial fibrillation.

Discussion

The antiarrhythmic drugs currently in clinical use target various ion channels or β-adrenergic receptors (41, 47, 48), but curiously, none of these enhances I_{Ks}, although the I_{Ks} channel is important in controlling the APD in the heart. In the physiological response to fight or flight, heart rate accelerates and I_{Ks} increases to shorten APDs, maintaining stable electrical activity and sufficient diastolic refilling (49). On the other hand, mutations in the I_{Ks} channel subunits, KCNQ1 and KCNE1, predispose patients to multiple types of cardiac arrhythmias (50) such as LQTS (51), short QT syndrome (52), and atrial fibrillation (46). In this study, molecular docking studies indicate that a shift of voltage-dependent activation of I_{Ks} to more negative voltages is desirable for antiarrhythmic effects, with minimal impact on the normal APD (*SI Appendix*, Fig. S5). We used in silico screening that targeted the VSD of KCNQ1 to identify C28, which was shown experimentally to shift voltage dependence of I_{Ks} activation to more negative voltages and enhance current amplitude (Figs. 1–6). C28 is specific in modulating I_{Ks} VSD activation and effective in preventing drug-induced APD prolongation or reversing it toward normal in ventricular myocytes (Fig. 6). Importantly, C28 shows smaller or negligible effects on APD of normal myocytes from both ventricle and atrium (Fig. 6).

For our in silico screening, we used the KCNQ1 VSD as a target in the hope that the compound docking to the site would directly affect VSD activation. Several lines of evidence validated that C28 is such a compound. We found that C28 shifts voltage dependence of KCNQ1 and I_{Ks} opening (Figs. 1 and 2). C28 interferes with the interactions of the gating charge with local environment during charge movements and shifts voltage dependence of VSD activation to more negative voltages (Fig. 3). C28 modulation is portable with the KCNQ1 VSD when it is fused with the nonvoltage-sensitive, two-pore–domain channel TASK3 (Fig. 4). Mutations of the amino acids that were predicted to interact with C28 in the in silico screening reduced C28 modulation (Fig. 4). Our conclusion that the shift of voltage dependence in KCNQ1 and I_{Ks} activation in C28 is primarily due to the C28-induced shift of voltage-dependent VSD activation is based on 1) the VCF measurements (Fig. 3*E*) and 2) the result that C28 no longer exhibits an effect on KCNQ1 activation when the VSD is arrested by mutations in the intermediate state (Fig. 5 *C* and *D*). The quantitative relation between the shifts in voltage dependence of VSD activation and pore opening might not be determined precisely because of a possible interaction between C28 and the fluorophore (Fig. 3*C*). For the I_{Ks} channels, C28 also causes an additional current enhancement (Fig. 2 *A* and *B*) by increasing the VSD–pore coupling (Fig. 5 *A* and *B*). Our study also showed that, although the VSDs in all voltage-gated ion channels share a similar structure, C28 is specific for KCNQ1 VSD activation in ventricular myocytes (Figs. 4 and 6 and *SI Appendix*, Figs. S2, S6, and S8). These results indicate that the KCNQ1 VSD can be used as a drug target to develop antiarrhythmic drugs.

In our study, the AP in GP ventricular myocytes were prolonged by Moxi and PI-103, which alter multiple cardiac ion channels to cause aLQTS (22). C28 effectively prevented or reversed these effects of the LQT-causing drugs (Fig. 6 *C* and *D*), supporting the hypothesis that increasing I_{Ks} can correct heart rhythm disturbed by changing other ion channels. Drugs approved to treat arrhythmias by blocking specific ion channels lack in efficacy and also have significant proarrhythmic potential (20, 53). For ventricular tachyarrhythmias in particular, antiarrhythmic drug therapy may be contraindicated (54). C28 enhances I_{Ks} to show antiarrhythmic effects, which indicates a mechanism on a new target for antiarrhythmic drug development. Importantly, our study shows that C28 has prominent features for cardiac safety. First, C28 affects APD in ventricular myocytes more prominently when it is abnormally prolonged than in control conditions (Fig. 6 and *SI Appendix*, Figs. S5 and S8). Second, C28 specifically activates the KCNQ1 VSD and has little effect on the voltage dependence or current of other ion channels that are important in shaping ventricular AP (Fig. 4 and *SI Appendix*, Figs. S6 and S8). The specificity of C28 will exclude off-target effects that may adversely alter heart rhythm. Third, C28 has small effects on atrial APD (Fig. 6), reducing the risk of atrial fibrillation as a side effect. These safety features of C28 are encouraging, considering the low concentration required for antiarrhythmic effects, which ranges from 1 to 100 nM in GP ventricular myocytes (Fig. 6). At these concentrations, C28 did not alter currents other than I_{Ks}, or APD in ventricular, or atrial myocytes (Fig. 6 and *SI Appendix*, Fig. S8).

These results describe the development and efficacy of a lead compound for the treatment of congenital or aLQTS. The results are significant, if this approach leads to a drug that can treat congenital and aLQT, for various reasons. 1) The arrhythmia TdP is often lethal. 2) The approach would eliminate an enormous expense in developing new drugs for any therapeutic application because of the Food and Drug Administration requirement that all new drugs minimize risk of aLQT. 3) It would result in greater efficacy for existing drugs by eliminating current dose restrictions induced by the aLQT side effect. In summary, it would dramatically reduce the cost of drug development, expand current drug efficacy, and save lives.

At present, the ion channels contributing to the function of many specific cells, the diseases associated with ion channel dysfunction in excitable and some nonexcitable tissues, the atomistic structures of ion channel families, and the molecular mechanisms of ion channel function are being elucidated at a rapid pace. Meanwhile, more powerful computational hardware and algorithms are also being developed at an increasing speed. This progress may provide a unique opportunity for rationally designed strategies for drug screening and development. This study provides an example to demonstrate the effectiveness of this approach.

Materials and Methods

C28 was identified by screening a compound library using molecular docking software and the structure model of the KCNQ1 channel and subsequently testing the effects of the compound on the currents of KCNQ1 and I_{Ks} expressed in *Xenopus* oocytes. In the oocytes, we used the two-electrode voltage clamp and VCF to study the functional effects and molecular mechanism of the action of C28 on KCNQ1 and I_{Ks} channels. The effects of C28 on I_{Ks} were examined in freshly isolated GP ventricular myocytes, while cardiac APs were recorded from both GP ventricular and atrial myocytes using the patch clamp technique. Detailed methods can be found in *SI Appendix, Supplementary Materials*.

Data Availability. All study data are included in the article and/or *SI Appendix*.

ACKNOWLEDGMENTS. We thank Zhaobin Gao for providing the complementary DNA of KTQ and KTV fusion proteins. Nien-Du Yang at Washington University helped in some experiments and data analyses. This work was supported by Grants R01 HL126774 (J.C., X.Z., and I.S.C.), R01 DK108989 (I.S.C.), R01 GM109980 (X.Z.), and R35GM136409 (X.Z.) from NIH and 13GRNT16990076 (X.Z. and J.S.) from the American Heart Association (Midwest Affiliate). Y. Lin was a visiting student supported by the China Scholarship Council (201206380052) via the Sixth Affiliated Hospital of Sun Yat-sen University, China; S.Z.G. was also supported through the National Library of Medicine Biomedical Informatics Research Training Program T15 LM07089. The computations were performed on the high-performance computing (HPC) infrastructure supported by the NSF Division of Computer and Network Systems 1429294 (PI: Chi-Ren Shyu) and the HPC resources supported by the University of Missouri Bioinformatics Consortium.

1. J. Silva, Y. Rudy, Subunit interaction determines IKs participation in cardiac repolarization and repolarization reserve. *Circulation* **112**, 1384–1391 (2005).Correction in: *Circulation* **120**, e84 (2009).
2. M. T. Keating, M. C. Sanguinetti, Molecular and cellular mechanisms of cardiac arrhythmias. *Cell* **104**, 569–580 (2001).
3. H. S. Wang, B. S. Brown, D. McKinnon, I. S. Cohen, Molecular basis for differential sensitivity of KCNQ and I(Ks) channels to the cognitive enhancer XE991. *Mol. Pharmacol.* **57**, 1218–1223 (2000).
4. Y. Li *et al*., KCNE1 enhances phosphatidylinositol 4,5-bisphosphate (PIP2) sensitivity of IKs to modulate channel activity. *Proc. Natl. Acad. Sci. U.S.A.* **108**, 9095–9100 (2011).
5. J. Barhanin *et al*., K(V)LQT1 and lsK (minK) proteins associate to form the I(Ks) cardiac potassium current. *Nature* **384**, 78–80 (1996).
6. M. C. Sanguinetti *et al*., Coassembly of K(V)LQT1 and minK (lsK) proteins to form cardiac I(Ks) potassium channel. *Nature* **384**, 80–83 (1996).
7. J. Sun, R. MacKinnon, Cryo-EM structure of a KCNQ1/CaM complex reveals insights into congenital long QT syndrome. *Cell* **169**, 1042–1050.e9 (2017).
8. J. Sun, R. MacKinnon, Structural basis of human KCNQ1 modulation and gating. *Cell* **180**, 340–347.e9 (2020).
9. D. Wu *et al*., State-dependent electrostatic interactions of S4 arginines with E1 in S2 during Kv7.1 activation. *J. Gen. Physiol.* **135**, 595–606 (2010).
10. K. C. Taylor *et al*., Structure and physiological function of the human KCNQ1 channel voltage sensor intermediate state. *eLife* **9**, e53901 (2020).
11. R. Barro-Soria *et al*., KCNE1 divides the voltage sensor movement in KCNQ1/KCNE1 channels into two steps. *Nat. Commun.* **5**, 3750 (2014).
12. P. Hou *et al*., Two-stage electro-mechanical coupling of a K_V channel in voltage-dependent activation. *Nat. Commun.* **11**, 676 (2020).
13. M. A. Zaydman *et al*., Kv7.1 ion channels require a lipid to couple voltage sensing to pore opening. *Proc. Natl. Acad. Sci. U.S.A.* **110**, 13180–13185 (2013).
14. J. D. Osteen *et al*., KCNE1 alters the voltage sensor movements necessary to open the KCNQ1 channel gate. *Proc. Natl. Acad. Sci. U.S.A.* **107**, 22710–22715 (2010).
15. J. Cui, Voltage-dependent gating: Novel insights from KCNQ1 channels. *Biophys. J.* **110**, 14–25 (2016).
16. J. M. Nerbonne, R. S. Kass, Molecular physiology of cardiac repolarization. *Physiol. Rev.* **85**, 1205–1253 (2005).
17. A. L. George Jr, Recent genetic discoveries implicating ion channels in human cardiovascular diseases. *Curr. Opin. Pharmacol.* **15**, 47–52 (2014).
18. P. J. Schwartz *et al*., Inherited cardiac arrhythmias. *Nat. Rev. Dis. Primers* **6**, 58 (2020).
19. H. L. Greene, Drug recalls underscore safety concerns. *Health News* **6**, 4 (2000).
20. D. M. Roden, Drug-induced prolongation of the QT interval. *N. Engl. J. Med.* **350**, 1013–1022 (2004).
21. C. Oshiro, C. F. Thorn, D. M. Roden, T. E. Klein, R. B. Altman, KCNH2 pharmacogenomics summary. *Pharmacogenet. Genomics* **20**, 775–777 (2010).
22. Z. Lu *et al*., Suppression of phosphoinositide 3-kinase signaling and alteration of multiple ion currents in drug-induced long QT syndrome. *Sci. Transl. Med.* **4**, 131ra50 (2012).
23. I. S. Cohen, R. Z. Lin, L. M. Ballou, Acquired long QT syndrome and phosphoinositide 3-kinase. *Trends Cardiovasc. Med.* **27**, 451–459 (2017).
24. J. J. Salata *et al*., A novel benzodiazepine that activates cardiac slow delayed rectifier K+ currents. *Mol. Pharmacol.* **54**, 220–230 (1998).
25. S. I. Liin *et al*., Polyunsaturated fatty acid analogs act antiarrhythmically on the cardiac IKs channel. *Proc. Natl. Acad. Sci. U.S.A.* **112**, 5714–5719 (2015).
26. V. Matschke *et al*., The natural plant product rottlerin activates Kv7.1/KCNE1 channels. *Cell. Physiol. Biochem.* **40**, 1549–1558 (2016).
27. G. Seebohm, M. Pusch, J. Chen, M. C. Sanguinetti, Pharmacological activation of normal and arrhythmia-associated mutant KCNQ1 potassium channels. *Circ. Res.* **93**, 941–947 (2003).
28. S. I. Liin, S. Yazdi, R. Ramentol, R. Barro-Soria, H. P. Larsson, Mechanisms underlying the dual effect of polyunsaturated fatty acid analogs on Kv7.1. *Cell Rep.* **24**, 2908–2918 (2018).
29. L. M. Boland, M. M. Drzewiecki, Polyunsaturated fatty acid modulation of voltage-gated ion channels. *Cell Biochem. Biophys.* **52**, 59–84 (2008).
30. A. Goel *et al*., Fish, fish oils and cardioprotection: Promise or fish tale? *Int. J. Mol. Sci.* **19**, 3703 (2018).
31. Y. Liu *et al*., A PIP_2 substitute mediates voltage sensor-pore coupling in KCNQ activation. *Commun. Biol.* **3**, 385 (2020).
32. C. Yan, X. Zou, "MDock: An ensemble docking suite for molecular docking, scoring and *in silico* screening" in *Computer-Aided Drug Discovery*, W. Zhang, Ed. (Springer New York, New York, NY, 2016), pp. 153–166.
33. S.-Y. Huang, X. Zou, An iterative knowledge-based scoring function to predict protein-ligand interactions: I. Derivation of interaction potentials. *J. Comput. Chem.* **27**, 1866–1875 (2006).
34. X. Xu, Z. Ma, R. Duan, X. Zou, Predicting protein-ligand binding modes for CELPP and GC3: Workflows and insight. *J. Comput. Aided Mol. Des.* **33**, 367–374 (2019).
35. P. Hou *et al*., Inactivation of KCNQ1 potassium channels reveals dynamic coupling between voltage sensing and pore opening. *Nat. Commun.* **8**, 1730 (2017).
36. M. A. Zaydman *et al*., Domain-domain interactions determine the gating, permeation, pharmacology, and subunit modulation of the IKs ion channel. *eLife* **3**, e03606 (2014).
37. P. Hou, J. Shi, K. M. White, Y. Gao, J. Cui, ML277 specifically enhances the fully activated open state of KCNQ1 by modulating VSD-pore coupling. *eLife* **8**, e48576 (2019).
38. X. Lan *et al*., Grafting voltage and pharmacological sensitivity in potassium channels. *Cell Res.* **26**, 935–945 (2016).
39. Y. Kim, H. Bang, D. Kim, TASK-3, a new member of the tandem pore K(+) channel family. *J. Biol. Chem.* **275**, 9340–9347 (2000).
40. D. Wu, H. Pan, K. Delaloye, J. Cui, KCNE1 remodels the voltage sensor of Kv7.1 to modulate channel function. *Biophys. J.* **99**, 3599–3608 (2010).
41. C. Antzelevitch, A. Burashnikov, Overview of basic mechanisms of cardiac arrhythmia. *Card. Electrophysiol. Clin.* **3**, 23–45 (2011).
42. P. Zimetbaum, Antiarrhythmic drug therapy for atrial fibrillation. *Circulation* **125**, 381–389 (2012).
43. H. S. Wang *et al*., KCNQ2 and KCNQ3 potassium channel subunits: Molecular correlates of the M-channel. *Science* **282**, 1890–1893 (1998).
44. A. E. Lacerda, J. Kramer, K.-Z. Shen, D. Thomas, A. M. Brown, Comparison of block among cloned cardiac potassium channels by non-antiarrhythmic drugs. *Eur. Heart J. Suppl.* **3** (suppl. K), K23–K30 (2001).
45. H. Morita, J. Wu, D. P. Zipes, The QT syndromes: Long and short. *Lancet* **372**, 750–763 (2008).
46. Y.-H. Chen *et al*., KCNQ1 gain-of-function mutation in familial atrial fibrillation. *Science* **299**, 251–254 (2003).
47. J. C. Estrada, D. Darbar, Clinical use of and future perspectives on antiarrhythmic drugs. *Eur. J. Clin. Pharmacol.* **64**, 1139–1146 (2008).
48. J. R. Hume, A. O. Grant, "Agents used in cardiac arrhythmias" in *Basic & Clinical Pharmacology, 13e*, B. G. Katzung, A. J. Trevor, Eds. (McGraw-Hill Medical, New York, NY, 2015), pp. 224–248.
49. N. Jost *et al*., Restricting excessive cardiac action potential and QT prolongation: A vital role for IKs in human ventricular muscle. *Circulation* **112**, 1392–1399 (2005).
50. L. Chen, K. J. Sampson, R. S. Kass, Cardiac delayed rectifier potassium channels in health and disease. *Card. Electrophysiol. Clin.* **8**, 307–322 (2016).
51. Q. Wang *et al*., Positional cloning of a novel potassium channel gene: KVLQT1 mutations cause cardiac arrhythmias. *Nat. Genet.* **12**, 17–23 (1996).
52. C. Bellocq *et al*., Mutation in the KCNQ1 gene leading to the short QT-interval syndrome. *Circulation* **109**, 2394–2397 (2004).
53. D. P. Zipes, Antiarrhythmic therapy in 2014: Contemporary approaches to treating arrhythmias. *Nat. Rev. Cardiol.* **12**, 68–69 (2015).
54. G. Frommeyer, L. Eckardt, Drug-induced proarrhythmia: Risk factors and electrophysiological mechanisms. *Nat. Rev. Cardiol.* **13**, 36–47 (2016).
55. B. Webb, A. Sali, Comparative protein structure modeling using MODELLER. *Curr. Protoc. Bioinformatics* **54**, 5.6.1–5.6.37 (2016).